



Impact toughness and fracture analysis of linear friction welded Ti–6Al–4V alloy joints

T.J. Ma, W.-Y. Li *, S.Y. Yang

Shaanxi Key Laboratory of Friction Welding Technologies, School of Materials Science and Engineering, Northwestern Polytechnical University, Xi'an, 710072 Shaanxi, PR China

ARTICLE INFO

Article history:

Received 21 June 2008

Accepted 20 August 2008

Available online 30 August 2008

Keywords:

Linear friction welding
Ti–6Al–4V titanium alloy
Impact toughness
Fracture analysis

ABSTRACT

Linear friction welding (LFW), as a relatively new solid-state joining technique, has great potentials in welding of non-axisymmetric components, especially for cost-effectively machining blade/disc (blisks) assemblies. In this study, Ti–6Al–4V alloy was jointed by the LFW process under the appropriate processing parameters developed before. The microstructure, impact toughness and fracture characteristics of LFW Ti–6Al–4V joint were investigated. The results showed that a sound weld was obtained consisting of a superfine $\alpha + \beta$ microstructure in the weld center (about 70 μm thickness). The weld presents a higher impact toughness ($61.3 \pm 5.8 \text{ J/cm}^2$) than the parent Ti–6Al–4V because of the superfine microstructure formed in the weld. The fracture surface exhibits three typical regions: the thin fibrous zone close to the notch, the radiation zone in the middle and the shear lip zone at the other three sides, corresponding to the crack initiation, propagation and shear failure zones, respectively. The crack develops a short distance along the weld center and thermomechanically affected zone after its initiation, and then extends into the parent metal due to the lowest impact toughness of the parent.

© 2008 Elsevier Ltd. All rights reserved.

1. Introduction

Linear friction welding (LFW) is a relatively new solid-state bonding process aiming at extending the current applications of rotary friction welding (RFW) to non-axisymmetric components. LFW involves joining of materials through the relative reciprocating motion of two components under an axial force as schematically shown in Fig. 1. LFW is observed to have four distinct phases, including the initial phase, the transition phase, the equilibrium phase, and the deceleration (or forging) phase [1,2]. During LFW, the frictional heat is generated and results in a continued plasticization of the interfacial region between the components. A flash is formed through the displacement of plastically deformed materials toward the weld edges. Once a sufficient plasticization has occurred, a forging force is applied, to produce a consolidated joint seam with the limited thermomechanically affected zone (TMAZ) and heat affected zone (HAZ). Although available for more than 15 years, LFW has only found the industrial application in aircraft engine manufacture, in part due to the high cost of the welding machines. LFW has proved to be an ideal process for joining turbine blades to discs where the high value-added cost of the components justifies the cost of a LFW machine. This approach is more cost-effective than machining blade/disc (blisks) assemblies from solid billets. LFW has been used successfully to join a range

of materials including titanium alloys [1–6], steels [7,8], intermetallic materials, aluminium, nickel, copper, and even dissimilar material combinations with the emphasis on aircraft engine alloys [9]. Although LFW has great application potentials in industries, there are few research reports available on LFW except some pioneer works [1–8]. Therefore, a large amount of research work is required to develop both scientific and practical knowledge of LFW.

The previous studies showed that a sound weld of titanium alloys with the refinement of microstructure could be obtained by LFW [1–6]. The weld presented a much higher hardness [3–5], and slightly better tensile properties [4,5] than the parent titanium alloys owing to the refined structure. In addition, the impact toughness of joints will be more important in applications for aerospace engines. However, few reports focused on this topic. Hence, the objective of the present work was to investigate the impact toughness of LFW Ti–6Al–4V alloy joints and their fracture characteristics.

2. Experimental procedures

Ti–6Al–4V blocks with a configuration of 10 mm width (W), 17 mm length (L) and 45 mm height (H) were welded in the plane $W \times L$. The typical microstructure of parent Ti–6Al–4V consists of a bimodal $\alpha + \beta$ structure in the form of elongated α grains (dark gray) and intergranular mixture of lamellar α and β grains (Fig. 2). A LFW machine (XMH-160) developed in Northwestern Polytechnical University (China) was employed to weld Ti–6Al–4V blocks. According to many preliminary experiments during

* Corresponding author. Tel.: +86 29 88460673; fax: +86 29 88491426.

E-mail addresses: liwy@nwpu.edu.cn, wenyali_cn@hotmail.com (W.-Y. Li).

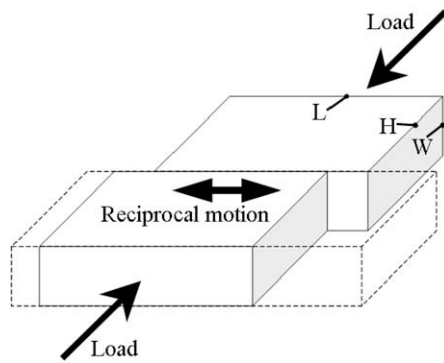


Fig. 1. Schematic of the LFW process.

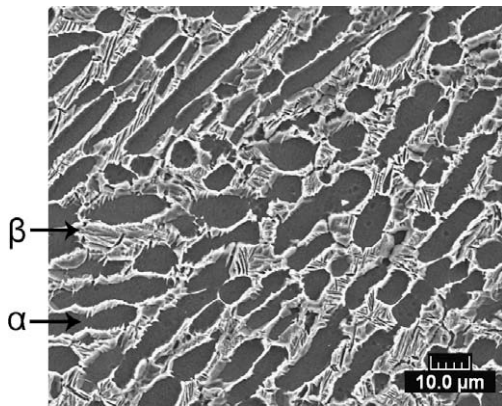


Fig. 2. SEM micrograph of parent Ti-6Al-4V alloy.

the development of the used welding machine, it was found that the friction time was the important factor as the appropriate force, frequency and amplitude were applied [7]. Through an observation of flashes of the joints obtained at different friction times, a good formability of flash and appropriate axial shortening were obtained for LFW Ti-6Al-4V at around 8 s. Therefore, the appropriate welding parameters were fixed as shown in Table 1. Five samples

Table 1
LFW parameters used in this study

Frequency (Hz)	33
Amplitude (mm)	4
Friction force (kN)	17.9
Friction time (s)	8
Forging force (kN)	36.8
Forging time (s)	4

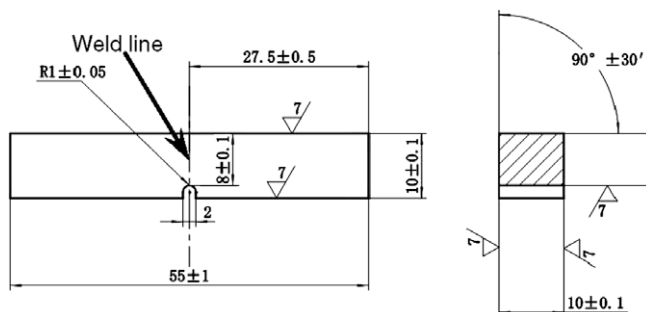


Fig. 3. Configuration and size of impact test specimen according to standard Mesnager U-notch Impact (GB/T229-1994).

were made for the impact test and one for the metallographic analysis.

The configuration and size of impact test specimens are shown in Fig. 3. The Mesnager U-notch specimens were machined from the welded blocks. A drop-hammer impact testing machine (JD-300B, Wuzhong Materials Testing Machine Co. Ltd., Ningxia, China) was used to measure the impact toughness of joints at room temperature. The specimens were polished on one lateral side and etched by a solution of 100 ml H₂O + 3 ml HF + 6 ml HNO₃ before machining the U-notch for the precise alignment of the weld line in the center of U-notch.

The joint macrostructure was observed by a digital camera. The microstructure of the joint cross-section (etched) was examined by scanning electron microscope (SEM), as well as the fractography.

3. Results and discussion

3.1. General features of LFW Ti-6Al-4V joint

Fig. 4 shows the typical macro photo and microstructure of LFW Ti-6Al-4V joint under the present welding conditions. From a visual inspection of the weld interface, an obvious flash from all sides of the joint was observed as illustrated in Fig. 4a. The flash is comprised of many ridges, which are generated as a result of the oscillating extrusion process during welding. This is the typical phenomenon in LFW and sometimes reflects the quality of weld. The axial shortening of five samples was estimated to be about 5 mm, which is enough to form a sound weld according to the results by Vairis and Frost [1]. It is clearly seen from Fig. 4b that a good weld was formed including the weld center of about 70 μm thickness and the thin TMAZ close to that. The superfine α + β microstructure was presented in the weld center, which contributes to the higher microhardness and tensile strength of joint compared to the parent metal [5]. In addition, the highly deformed α and β-phases oriented along the deformation direction were ob-

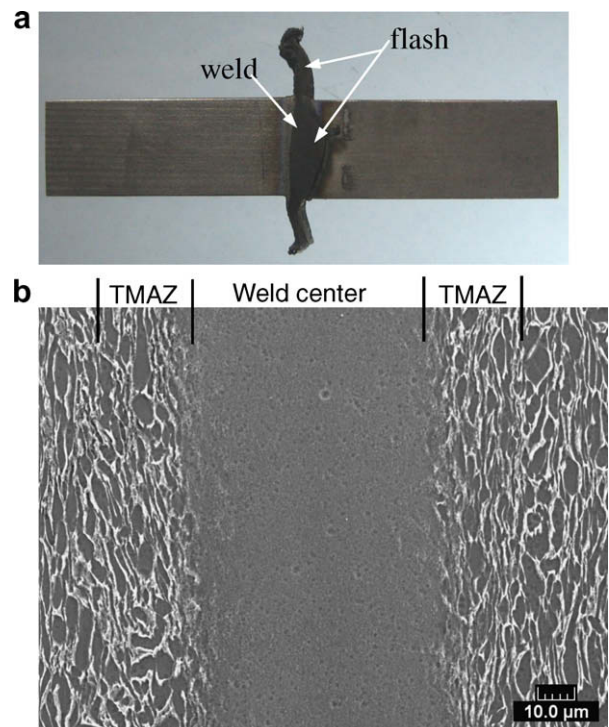


Fig. 4. (a) Macro photo, and (b) Microstructure of LFW Ti-6Al-4V joint under the present welding conditions.

served in TMAZ. It was also found that the HAZ was much limited and could not be determined in this study because of the structure stability of Ti–6Al–4V under a temperature lower than 600–800 °C [5]. All these results are associated with the short thermal history, which the interfacial materials experienced during LFW.

The average power input (PI) during LFW for the developed machine can be characterized as [5]

$$PI = 4\mu fap \quad (1)$$

where μ is the average coefficient of friction, f and a are the frequency and amplitude of oscillation, respectively. P is the friction pressure defined as the ratio of friction force to the cross-sectional area of specimen. The preliminary thermal modeling indicated that the interface temperature could be quickly increased to higher than 1000 °C compared to that of 980 ± 10 °C for $\alpha + \beta \leftrightarrow \beta$ temperature of Ti–6Al–4V. Vairis et al. [1,2] and Wanjara et al. [4] also indicated that the peak interface temperature exceeded the β -transus temperature. Owing to poor thermal conductivity of Ti–6Al–4V, the final high temperature region (>900 °C) is limited in about ± 2 mm around the weld center line.

3.2. Impact toughness and failure characteristics

Table 2 shows the results on the impact toughness of joints. The impact toughness is characterized by α_k , a value defined through dividing the impact energy (A_k) by the minimum cross-sectional area of the starting sample. The results yield an average value of 61.3 ± 5.8 J/cm². The observation of the fractured surfaces clearly shows that all the failures occurred in the parent metal (Fig. 5). This fact suggests that the impact toughness of the weld is higher than that of the parent metal. It is also found that Sample 2 presents the lowest value (52 J/cm²) and Sample 3 the highest (67.1 J/cm²). The observation of the fractured surfaces and cracks shows that the crack initiation, propagation and shear failure totally occurred in the parent metal for Sample 2 (Fig. 5a). But for Sample 3 (Fig. 5b), the crack initiated in the weld center, and quickly propagated through the TMAZ into the parent metal, finally the fracture occurred in the parent metal. The fracture features of Samples 1, 4 and 5 are similar to that of Sample 3. Therefore, it could be considered that the misalignment of the weld line with the U-notch center during machining the U-notch may attribute to the relatively low impact toughness of Sample 2 taking into account the fact that the parent metal presents a lower impact toughness compared to the weld.

For a better understanding of the underlying mechanisms, the failure features were analyzed in detail taking Sample 3 as an

example. It is found that the fracture surface presents three typical regions, i.e., the thin fibrous zone close to the notch, the radiation zone in the middle and the shear lip zone at the other three sides, respectively, corresponding to the zones marked by A, B and D as shown in Fig. 6a. This fact is consistent with the results on RFW Ti–6.5Al–1.9Zr–3.3Mo–0.25Si joint [10]. In addition, the crack initiation, propagation and shear failure just locate, respectively, at these three zones. It is seen that there are some tear ridges, cleavage planes and secondary cracks at the crack initiation point (bottom of Fig. 6b). The crack develops a short distance (0.3–0.5 mm) along the weld center and TMAZ after its initiation. In the weld center, as marked by arrow 1 in Fig. 6b, many fine dimples and tear ridges are formed presenting a typical ductile fracture (the right hand of Fig. 6b). In TMAZ (left-hand of Fig. 6b), the quasi-cleavage fracture is presented. Moreover, the cleavage fracture is presented in the crack initiation zone of the weld center owing to the fast loading rate during the impact test, as marked by arrow 2 in Fig. 6b. But an obvious plastic deformation and some secondary cracks are developed in this cleavage region because of the good ductility and well resistance to crack propagation of weld center with superfine structure. This will drive the crack to propagate into the parent metal.

In the crack propagation zone (Fig. 6c), a typical composite fracture of the quasi-cleavage and dimples is presented. Many tear ridges and deformed dimples are distributed around the brittle areas of the quasi-cleavage planes. As shown in Fig. 6e, the shear lip zone exhibits a typical ductile fracture with many fine dimples dispersed. However, at the border of crack propagation and shear lip zones as shown in Fig. 6d, evident tear ridges and secondary cracks are observed, which means a composite fracture of the cleavage, quasi-cleavage and dimples.

3.3. Discussion on fracture mechanism

According to above results, it is believed that the crack propagation into the parent metal is mainly associated with the joint microstructure and the corresponding properties. As reported by Balasubramanian et al. [11], a significant effect of grain size on impact toughness of pulsed current GTA welded Ti–6Al–4V joint was found. The impact strength lowers by a factor of about 50% or more with increasing the grain size from 100 μ m to about 550 μ m [11]. It is reported that the relation between the impact strength and the grain size usually follows the Hall–Petch relationship as follows [12]:

$$\sigma_c = K \cdot d^{-\frac{1}{2}} \quad (2)$$

where σ_c is the fracture stress, d is the grain size and K is a material constant. Other researchers also indicated that the relationship between the properties and grain sizes of $\alpha + \beta$ Ti alloys followed the empirical Hall–Petch expression [13,14]. According to the microstructure observation in this study, the average grain size of parent Ti–6Al–4V is about 40 μ m, while the grain size in the weld center is several microns [5], such as 4 μ m [4]. Therefore, a simple calculation indicates that the fracture stress of weld center will be about three times than that of the parent metal. The impact toughness values obtained in the present study indicate that the impact strength of weld center is higher than that of the parent metal. Therefore, it is quite reasonable that the crack propagates quickly and easily into the parent metal during the impact test. The results by Balasubramanian et al. [11] also follows the Hall–Petch relationship according to Eq. (2).

However, why the crack does not propagate along the TMAZ? According to the results reported by Karadge et al. [6], the texture of TMAZ in the LFW Ti–6Al–4V joint presented a much different structures, i.e., a dramatic change from almost random to strong transverse texture. This fact may be resulted from the fast defor-

Table 2
Impact toughness values of specimens (α_k)

Sample no.	1	2	3	4	5
α_k (J/cm ²)	60.1	52.0	67.1	62.4	64.9

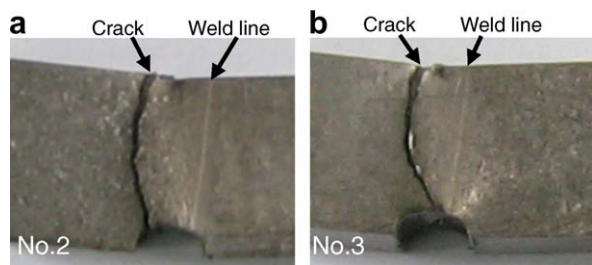


Fig. 5. Macrographs of the fractured samples after impact test. (a) Sample 2; and (b) Sample 3.

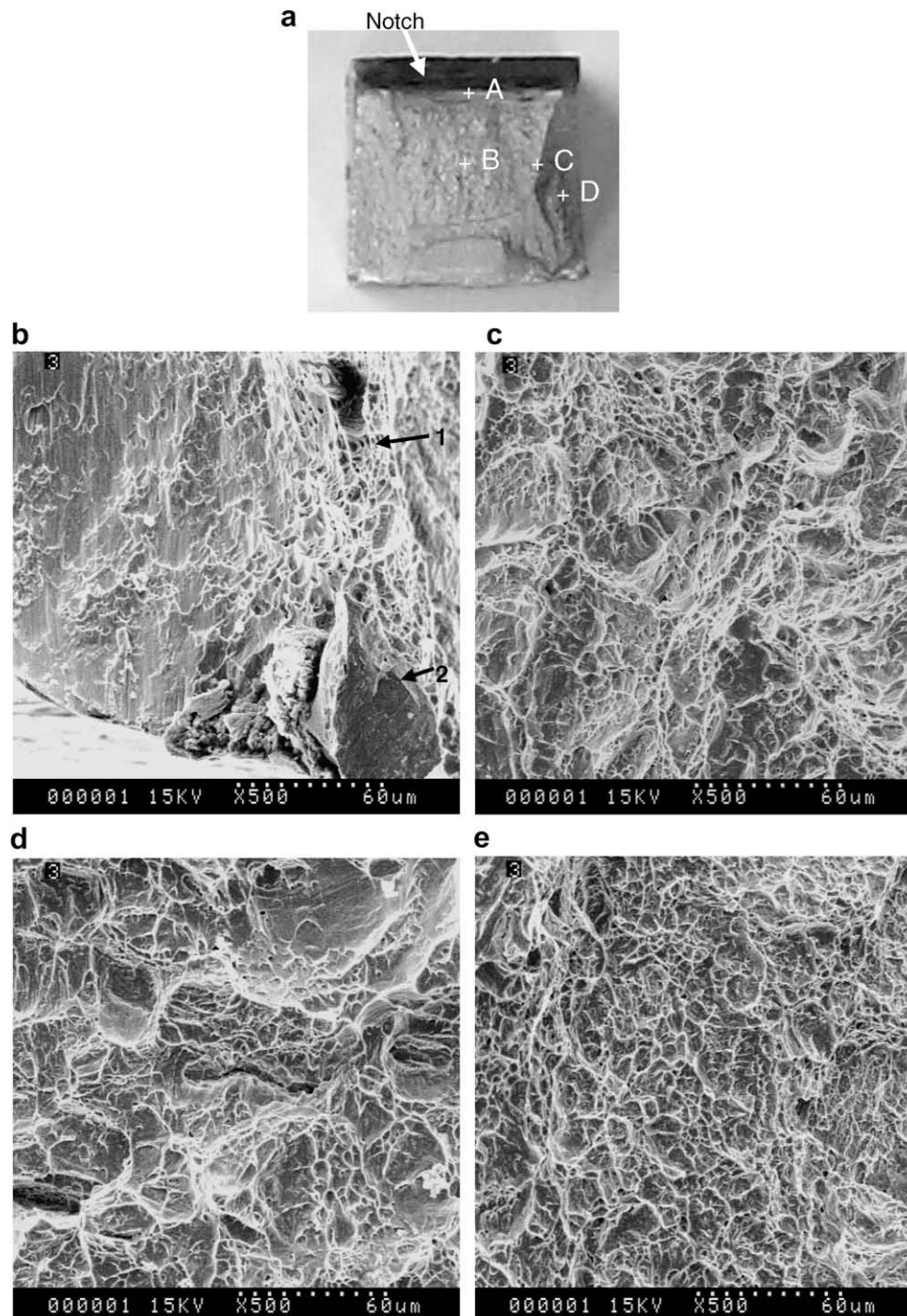


Fig. 6. Fractographs of Sample 3 observed on the left-hand part as shown in Fig. 5: (a) Macrograph; (b–e) micrographs corresponding to zones A–D, respectively, as marked in (a). (b) Crack initiation zone; (c) crack propagation zone; (d) border of crack propagation and shear lip zones; and (e) shear lip zone.

mation process near the β -transus temperature in this zone having a majority of β -phase [6]. Therefore, the unusual arrangement and orientation of crystals may improve the impact strength of this zone. Thus the parent metal will be the weakest zone for the crack to propagate. Future work is still needed to clearly reveal this phenomenon.

4. Conclusions

From the microstructural examination and the measurement of impact toughness of the LFW Ti–6Al–4V alloy joint, it was found

that the impact toughness of the weld was higher than that of the parent Ti–6Al–4V because of the superfine microstructure formed in the weld center. The average impact toughness of the samples was $61.3 \pm 5.8 \text{ J/cm}^2$. The fracture analysis shows that the fracture surface of the impacted specimen presents three typical regions: the thin fibrous zone close to the notch, the radiation zone in the middle and the shear lip zone at the other three sides, corresponding to the crack initiation, propagation and shear failure zones, respectively. The crack develops a short distance along the weld center and TMAZ after its initiation and extends quickly into the parent metal due to its lowest impact strength.

Acknowledgements

The authors would like to thank the financial support from National Aerospace Science Foundation (No. 20061153015). The author, Wenya LI, gratefully acknowledges the support of Youth for NPU Teachers Scientific and Technological Innovation Foundation and the Aoxiang Star Project.

References

- [1] Vairis A, Frost M. *Wear* 1998;217:117.
- [2] Vairis A, Frost M. *Mater Sci Eng A* 1999;271:477.
- [3] Baeslack III WA, Broderick TF, Juhas M, Fraser HL. *Mater Charact* 1994;33:357.
- [4] Wanjara P, Jahazi M. *Metall Mater Trans A* 2005;36:2149.
- [5] Ma TJ, Li WY, Xu QZ, Zhang Y, Li JL, Yang SQ, et al. *Adv Eng Mater* 2007;9:703.
- [6] Karadge M, Preuss M, Lovell C, Withers PJ, Bray S. *Mater Sci Eng A* 2007;459:182.
- [7] Li WY, Ma TJ, Xu QZ, Yang SQ, Zhang Y, Li JL, et al. *Mater Lett* 2008;62:293.
- [8] Li WY, Ma TJ, Zhang Y, Xu QZ, Li JL, Yang SQ, et al. *Adv Eng Mater* 2008;10:89.
- [9] Threadgill P. Linear friction welding, TWI Knowledge Summary. The Welding Institute, UK. <http://eurostir.co.uk/j32k/protected/band_3/ksplt001.html>.
- [10] Mohandas T, Banerjee D, Kutumba Rao VV. *Mater Sci Eng A* 2000;289:70.
- [11] Balasubramanian M, Jayabalan V, Balasubramanian V. *Mater Lett* 2008;62:1102.
- [12] Ha FK. The microcosmic theory of metal mechanics character. Beijing, China: Science Press; 1983.
- [13] Venkatramani G, Ghosh S, Mills M. *Acta Mater* 2007;55:3971.
- [14] Semiatin SL, Bieler TR. *Acta Mater* 2001;49:3565.